RESISTIVE DAMPING OF PULSE-SENSED CAPACITIVE POSITION SENSORS

By

Mathew Varghese

B.S. University of California, Berkeley (December 1994)

Submitted to the

Department of Electrical Engineering and Computer Science
in partial fulfillment of the requirements for the degree of

Master of Science

at the

Massachusetts Institute of Technology

February, 1998

Signature of Author.....
Department of Electrical Engineering and Computer Science
October 27, 1997

Certified by.....
Stephen D. Senturia, Barton L. Weller Professor
Department of Electrical Engineering and Computer Science
Thesis Supervisor

Accepted by.....
Arthur C. Smith
Department of Electrical Engineering and Computer Science
Chairman, Department Committee on Graduate Students

Resistive Damping of Pulse-Sensed Capacitive Position Sensors

Mathew Varghese

Submitted to the

Department of Electrical Engineering and Computer Science
on October 24, 1997 in partial fulfillment of the requirements for the degree of

Master of Science in Electrical Engineering and Computer Science

Abstract

The use of capacitance measurement to determine the position of an elastically supported plate, a method used in a variety of microelectromechanical sensors, is limited by the phenomenon known as pull-in. The voltage used to sense the capacitance applies a mechanical load, and if this voltage is too large, the measurement is seriously perturbed. Recently, a dynamic differential capacitive sensing scheme was proposed that uses a sense voltage much higher than the pull-in voltage. Short pulses that exceed the pull-in voltage are applied differentially to a sense capacitor and reference capacitor. The voltage that appears on their shared node during the sense pulse is proportional to the difference between the two capacitances. Because the pulses are applied for only a very short time, static pull-in does not occur. However, the pulses impart kinetic energy to the supported plate, and after the pulses are removed, the mechanical system can undergo oscillatory motion. This motion must be controlled in amplitude, and must be optimally damped so that the next sense measurement can be made as quickly as possible.

This thesis investigates the electromechanical dynamics of both the sense procedure and a proposed resistive damping method that permits effective damping even for devices that must operate in vacuum, and hence, cannot depend on squeeze-film damping. Resistive damping is a passive electronic method of damping mechanical oscillations, and is inherently non-linear. A one-dimensional model of a thermomechanical radiant energy sensor is used to illustrate the sensing and damping dynamics, and show how parameters for optimal damping are found. Additionally, a limit on the sensitivity of the differential-sensing scheme imposed by the resistive damping method is discussed. Experimental evidence of resistive damping is presented and compared to theory.

Thesis Supervisor: Stephen D. Senturia
Weller Professor of Electrical Engineering and Computer Science

Acknowledgments

The work done for a thesis is never a solitary effort. There are many people who significantly influence the outcome in a positive way by providing technical, financial, and moral support. I take this opportunity to thank them individually.

First and foremost, I want to thank my advisor Stephen Senturia for providing the guidance and funding necessary to complete my thesis. He buffered me from the financial issues that accompany research allowing me to focus on solving problems. His timely insights, critical reviews of my work, and gentle prodding are much appreciated, as are his travel tales.

I want to thank Bob Amantea and Don Sauer of the Sarnoff Corporation for presenting me with such an interesting problem to explore for my thesis. I spent an enjoyable summer working with Bob, and received advice on topics ranging from modeling techniques, to finding the right partner in life. The enthusiasm he brought to his work has rubbed off on me.

I want to thank Raj Gupta for bringing me up to speed when I started my graduate career, and Kush Gulati for his technical advice, but more for the hours we spent in speculative discussion on topics far beyond our understanding.

Finally, my parents, my brother, Zubin, and my girlfriend, Sharon, deserve a special thanks for their wisdom, love, and good humor during stressful times.

This work was sponsored, in part, by DARPA under contract J-FBI-95-215, and by the Sarnoff Corporation.

Table of Contents

CHAPTER 1

Introduction

Microelectromechanical sensors, such as accelerometers [1], pressure sensors [2,3], and thermomechanical radiant energy sensors [4], commonly use methods of differential capacitive sensing to measure the change in position of an elastically supported plate that moves in response to an applied stimulus. The voltage used to sense the capacitance can perturb the system and as a result must be kept below the pull-in voltage [6], limiting the sensitivity of the measurement. This limit is particularly important when the sensor has a low pull-in voltage. Amantea [4] proposed a dynamic differential capacitive sensing scheme in which short pulses that *exceed* the pull-in voltage are applied to a sense and reference capacitor. Because the pulses are kept short, pull-in is avoided.

An approximate lumped element model which illustrates the sensing mechanism is shown in Figure 2.2. The output is the voltage that appears on the sense plate. The sensitivity to capacitive imbalance between C_S and C_R is proportional to the applied voltage, and can exceed the quasi-static limit set by pull in. However, the pulses impart kinetic energy to the supported plate, and after the pulses are removed, the mechanical system can undergo oscillatory motion. This motion must be controlled in amplitude, so that the plate does not "crash" into the sense plate, and must be optimally damped so that the next sense measurement can be made as quickly as possible. Resistive damping [5] is proposed as a method of damping, but it places an additional limit on the sense voltage that can be applied, thereby limiting the sensitivity.

This thesis studies the dynamics of the pulsed capacitive sensing technique when it is used in conjunction with the resistive damping method. The objective is to determine how to choose parameters that optimize the damping, and additionally, determine what constraints resistive damping places on the pulsed capacitive sensing technique. Experimental results are presented that demonstrate the viability of this damping method.

1.1 Thesis Outline

This section describes the thermomechanical radiant energy sensor that was the motivation behind the work done for this thesis. Numerical examples throughout the thesis are based on nominal values for this sensor. In Chapter 2, a lumped element model of the sensing and damping schemes is introduced and used to derive a pair of coupled ordinary differential equations describing the electromechanical system. Simulations based on these equations are used to demonstrate the dynamics, chart out the design space, and determine the parameters for optimum damping. Experimental results are presented in Chapter 3 to demonstrate the viability of the damping mechanism. The experimental results are then compared to simulation based on the theory in Chapter 2. Chapter 4 summarizes the findings of this work, and presents an analysis of the merits and drawbacks of resistive damping when it is used in a pulsed capacitive sensing scheme.

1.2 Motivation

The pulsed capacitive sensing scheme was originally proposed by Amantea [4] for use in a thermomechanical radiant energy sensor. The sensor, shown schematically in Figures 1.1 and 1.2, consists of an elastically supported plate forming the top electrode of a capacitor, a bi-material strip, and a thermally isolating support. When IR radiation is focused onto the absorbing material on top of the plate, the plate heats up, and the resulting thermal energy flows to the bi-material strip and causes a temperature rise. The bi-material strip, made of two materials with mismatched thermal expansion coefficients, bends to alleviate the resulting stress built up along it's length. This in turn causes the plate to rise, changing a sense capacitance which is the measured quantity. The sensor must be fairly well thermally isolated from the substrate for optimum sensitivity, hence the insulative support. This requirement also forces the sensor to be operated under vacuum to prevent convective, and conductive heat losses through the surrounding air.

The sensor is part of a thermal imager that operates at television frame rates of about 30 frames per second, which means the change in capacitance due to IR radiation must be measured at least every 33ms. Thus, there is a minimum sampling rate restriction on the type of sensing technique that is used.

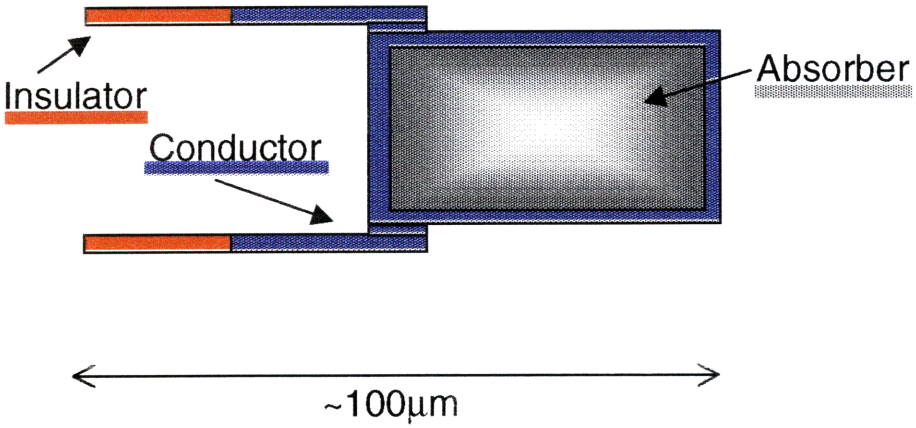

Figure 1.1: Top view of the thermomechanical radiant energy sensor.

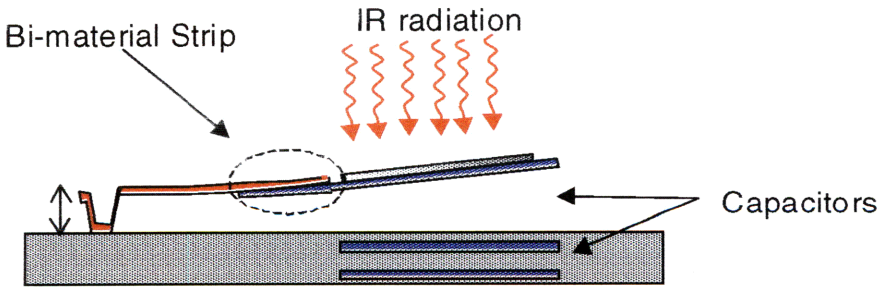

Figure 1.2: Side view of the thermomechanical radiant energy sensor.

CHAPTER 2

Theory and Simulation

This chapter begins with a description of a one dimensional lumped element model of a generic position sensor which forms the basis of the analysis in the rest of the chapter. The limitations of existing differential sensing schemes are described, the pulsed capacitive sensing technique is introduced, and the dynamics associated with this technique are explained. The resistive damping method is presented. The effect of resistive damping on the dynamics of the sensing technique and the resulting limitations placed on the sensor sensitivity are analyzed. Finally, simulations are carried out using the thermomechanical radiant energy sensor as an example to demonstrate a methodology to optimize a pulsed capacitive sensor when resistive damping is used.

2.1 Lumped Element Sensor Model

The analysis in this chapter is based on a one-dimensional lumped element model of a generic capacitive position sensor. The model assumes the position sensor consists of an elastically supported plate that moves in response to an applied stimulus. This plate forms one electrode of a sense capacitor C_S and this capacitance is sensed to detect any changes in the plate's position. Figure 2.1 illustrates the sensor model. The elastically supported plate is represented by a plate of mass m, and area A, suspended by a spring of stiffness K, a nominal distance h_0 above a sense plate. The supported plate and sense plate form a capacitor C_S that is a function of their separation x. The radiant energy sensor used in the examples in this thesis has nominal lumped element parameter values given in Table 2.1.

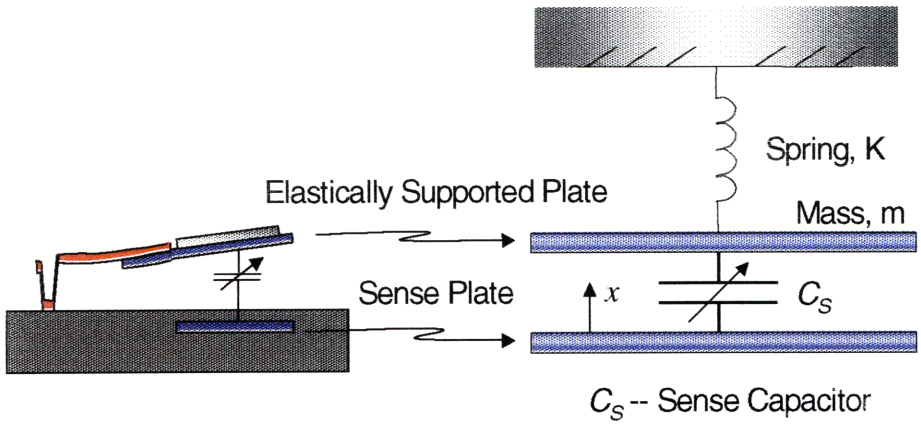

Figure 2.1: A 1-D lumped element model of a capacitive position sensor.

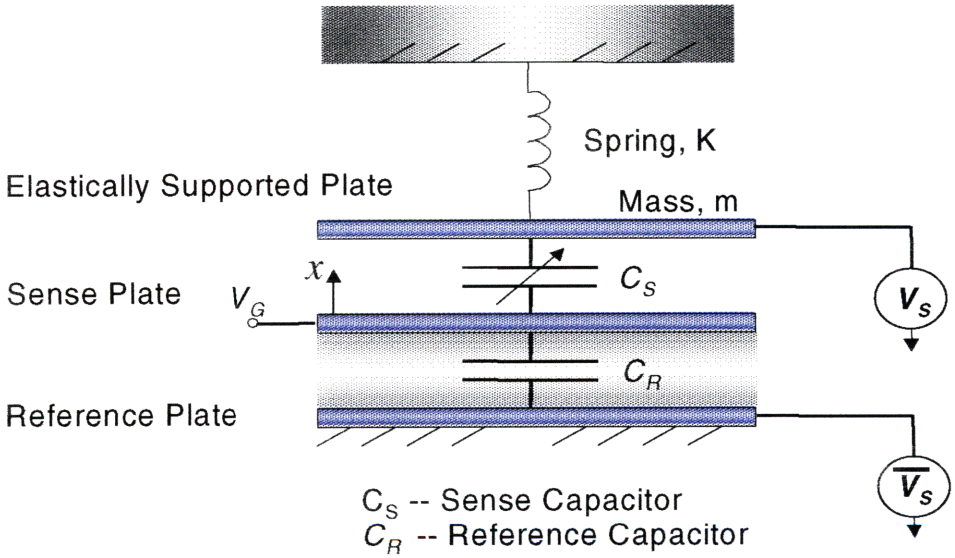

Figure 2.2: A generic capacitive position sensor in a differential measurement scheme.

Parameter	*K*	*m*	ω_0	h_0	*A*	C_{S0}, C_R
Value	**1.5mN/m**	**1.18ng**	**35700rad/sec**	**1670μm^2**	**0.54μm**	**27.3fF**

Table 2.1: Nominal lumped element parameters for the radiant energy sensor.

2.2 Differential Capacitive Sensing

There are numerous techniques for measuring changes in the sense capacitance, the most common of which use differential sensing where the sense capacitor is compared to a reference capacitor, with the output proportional to the difference between the two capacitors[1,2,3]. Differential sensing has the advantage of providing a linear output for small changes in the sense capacitance, with zero offset if the reference capacitor is chosen appropriately. However, the voltage or charge that is used to make a measurement also applies an electrostatic load to the sensing element, and if the load is large enough, the measurement is severely perturbed. This effectively places an upper limit on the sensitivity of the sensor.

Figure 2.2 shows the generic sensor in a differential measurement scheme, where a reference capacitor C_R is introduced. DC sense voltages V_S and $\overline{V}_S$ are applied to the sense capacitor and reference capacitor respectively. The voltage V_G that appears on their shared node is given by

$$V_G = \frac{V_S C_S + \overline{V}_S C_R}{(C_S + C_R)} = \frac{V_S \Delta C_S}{(C_S + C_R)} \tag{2.1}$$

if $\overline{V}_S$ and C_R are chosen such that

$$V_S C_{S0} = -\overline{V}_S C_R \tag{2.2}$$

where C_{S0} is the nominal sense capacitance $\varepsilon_0 A/h_0$. Thus, the sensitivity of this sensing technique scales with the sense voltage V_s, and mandates the use of as large a value as possible.

2.2.1 Static Pull-in Limit

If V_s is larger than the static pull-in voltage [6]

$$V_{PI} = \sqrt{\frac{8Kh_0^3}{27A\varepsilon_0}} \tag{2.3}$$

of the suspended plate, the electrostatic load causes the plate to collapse. Thus, V_S has an upper limit set by static pull-in. Most MEMS structures are designed so that this voltage is sufficiently high for the sensitivity requirements of the particular sensor. However, this

limit is a critical restriction for devices with low pull-in voltages, such as the thermomechanical radiant energy sensor that was the motivation behind this work. The radiant energy sensor has a pull-in voltage of 68mV.

2.3 Pulsed Capacitive Sensing

To boost sensitivity above the limit set by pull-in, Amantea proposed replacing the DC sense voltages with two pulses, V_S and $\overline{V}_S$, of magnitude *greater* than the pull-in voltage. The sensitivity of this measurement scheme is determined by the size of the applied sense pulses as the output voltage during the pulses is still given by Equation (2.1). Pull-in is prevented by keeping the duration of the pulses t_0 very short. This also insures that the change in capacitance due to the electrostatic load applied by the pulses is negligible compared to the change due to the measured stimulus during the pulses. However, significant kinetic energy is imparted to the supported plate during the pulses, and after the pulses are removed, the mechanical system can undergo oscillatory motion. This motion must be controlled in amplitude so that the plate does not "crash" into the sense plate, and must be optimally damped so that the next sense measurement can be made as quickly as possible.

2.3.1 Dynamics

We first consider the dynamics of the plate without any damping. The kinetic energy imparted to the supported plate during a pulse of width t_0 can be calculated under the assumption that the movement of the plate is negligible *during* the pulse. This is true if the duration of the pulse is kept short. The spring force is negligible as it is proportional to displacement, thus, only the electrostatic force F_E acts on the plate and is given by

$$F_E = \frac{1}{2}\frac{\varepsilon_0 A V_S^2}{x^2} \approx \frac{1}{2}\frac{\varepsilon_0 A V_S^2}{h_0^2} \tag{2.4}$$

where ε_0 is the permittivity of vacuum, A is the plate area, V_s is the pulse height, and h_0 is the nominal gap height. Following from this, the displacement d of the plate during the measurement is

$$d = \frac{1}{4}\frac{\varepsilon_0 A V_S^2 t_0^2}{h_0^2 m} \tag{2.5}$$

and it's kinetic energy KE is

$$KE = \frac{1}{8}\frac{\varepsilon_0^2 A^2 V_s^4 t_0^2}{h_0^4 m} \tag{2.6}$$

Note that the kinetic energy is a strong function of the size of the sense voltage V_s. The system behavior after the end of the pulse is that of an undamped oscillating mass-spring system. Referring to Figure 2.3, the maximum allowed V_S is calculated by setting the amplitude of the oscillation equal to the gap height h_0 so that the position x is always greater than zero, preventing the "crash" of the supported plate into the sense plate.

$$V_{S,\,max} = \sqrt{\frac{2\omega_0 h_0^3 m}{\varepsilon_0 A t_0}} \tag{2.7}$$

where ω_0 is the resonant frequency of the supported plate. $V_{S,max}$ for the radiant energy sensor is 3.0V for a pulse width of 0.1μs.. This is significantly higher than the sensor's pull-in voltage of 68mV.

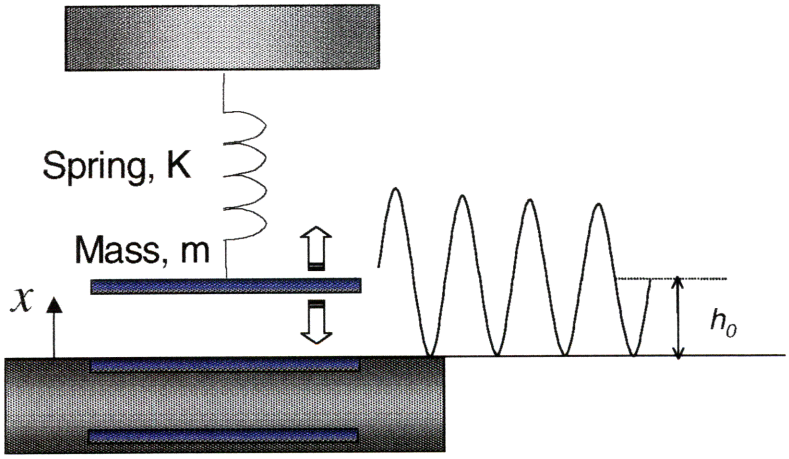

Figure 2.3: Free mechanical oscillations result after the plate is set in motion. The amplitude of these oscillations must be less than h_0 to prevent "crashing" the sensor.

2.4 Damping

In order to make another measurement the amplitude of the residual oscillations must be damped below the resolution of the sensor. This means that the time taken to damp oscillations determines the sampling rate of the sensor. Thus, the damping method plays a critical role in determining the sampling rate of pulsed capacitive sensors.

2.4.1 Squeeze Film Damping

It is possible to use compressible squeezed-film damping (CSQFD) [7] to damp the mechanical oscillations, and in fact this would actually allow us to *increase* V_S above the limit in Equation (2.7). This is because the motion of the supported plate is damped throughout the motion, hence the maximum amplitude of oscillation for a given sense pulse is lower than the undamped case. However, in situations where the sensing technique must be applied in vacuum, CSQFD is not possible and an alternative damping method must be used. The use of CSQFD damping is not investigated in this thesis.

2.4.2 Resistive Damping

Resistive damping is a method that damps the mechanical oscillations in the elastically supported plate even in vacuum. It is achieved by introducing a damping resistor R_D to which a DC voltage V_D is applied after the end of the sense pulse, as illustrated in Figure 2.4. It turns out that the damping produced by this resistor is highly nonlinear. This is seen by considering the direction of the electrostatic force on the supported plate relative to the direction of its motion. When the plate is moving up, the electrostatic force acts to retard the motion, whereas it accelerates the motion when the plate is moving down. In a linearly damped system, the damping force always acts to retard the motion. From an energy point of view this method works by transferring kinetic energy to electrostatic energy in the capacitors, and then dissipating this energy through joule heating in the resistor.

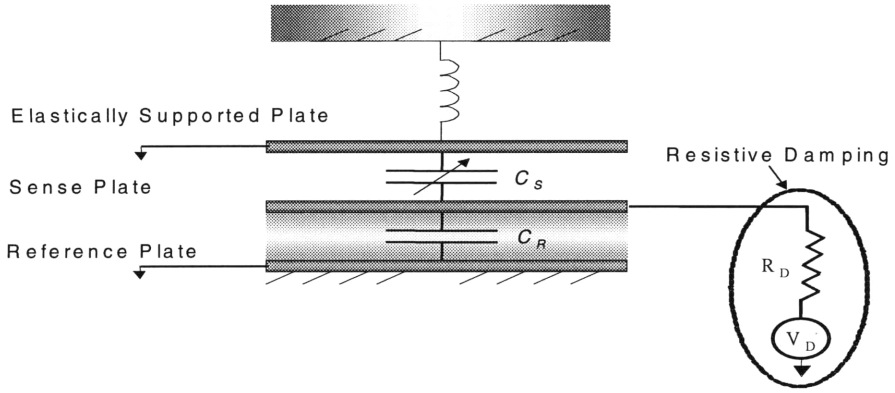

Figure 2.4: Resistive damping scheme consisting of a DC voltage source and a damping resistor.

Now consider the voltage at the sense plate V_G as the supported plate oscillates

$$V_G = \frac{Q(t)}{C_S(t) + C_R} \tag{2.8}$$

where Q(t) is the charge on the sense plate. The motion of the plate changes the total capacitance, which in turn raises or lowers V_G about the damping voltage V_D. From Figure 2.5, it is evident that when V_G rises above V_D, the capacitors discharge, and when it falls below V_D, the capacitors charge up. The resulting current flowing back and forth through the resistor dissipates energy.

The charge on the sense plate oscillates about its static value of $V_D/(C_S + C_R)$ and this oscillation is out of phase with the motion of the plate. Therefore the force on the plate, which is proportional to the square of the charge, is also out of phase with the motion of the plate, as shown in Figure 2.6. This means that the retarding force during the upward motion of the plate is greater than the accelerating force during the downward motion of plate -- the plate is retarded more than it is accelerated every cycle.

2.4.3 Damping Resistor

The size of the resistor plays an important part in this damping phenomenon. It is found, through simulation, that optimum damping is achieved when

$$R_D C_T \approx \frac{1}{\omega} \tag{2.9}$$

where ω is the angular frequency, and C_T is the total capacitance seen by the resistor. That is, the RC time constant of the electrical circuit has to match the period of oscillation divided by 2π.

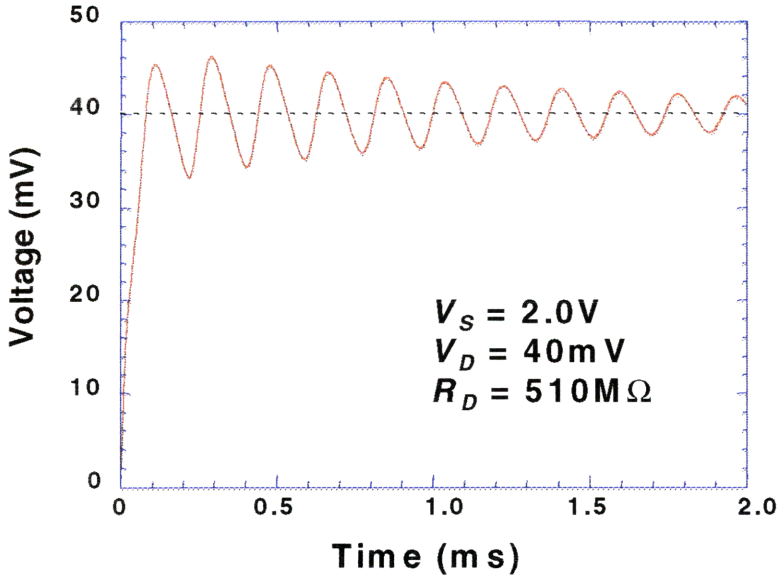

Figure 2.5: Voltage on the sense plate during damping. The voltage falls below and rises above the damping voltage of 40mV, charging and discharging the sense node, respectively.

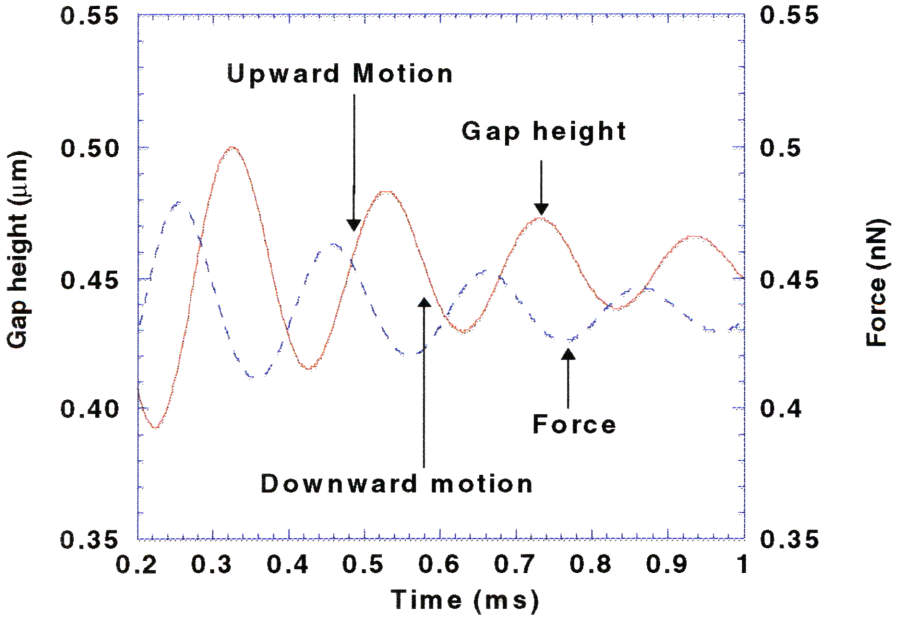

Figure 2.6: Graph of gap height and force during damping. Damping force is maximum during the upward motion of the plate, and minimum during the downward motion of the plate.

2.4.4 Damping Voltage

The DC voltage source V_D effectively acts as a source of charge for this damping mechanism. If the resistor was connected to ground, no damping would occur as the charge, and hence the electrostatic force, on the elastically supported plate would be zero. When V_D is increased, damping improves because the damping forces are larger, but V_D introduces limitations on the size of the sense pulse V_S.

For a given damping voltage, if the amplitude of mechanical oscillation is too large, the plate moves into a region where the non-linear electrostatic force overwhelms the spring force and causes the supported plate to collapse. This phenomenon is known as dynamic pull-in [8,9]. For a particular damping voltage, V_S must be kept below the value at which dynamic pull-in occurs which is *below* the limit given by Equation (2.7). Therefore, sensitivity is reduced.

Dynamic pull-in is best described by looking at the potential energy (Figure 2.7) of the supported plate in the limit R_D is small.

$$U(\Delta x) = \frac{1}{2}K\Delta x^2 - \frac{1}{2}\frac{\varepsilon_0 A V_D^2}{(h_0 - \Delta x)} \tag{2.10}$$

Δx is the displacement from the supported plate's nominal position. Initially, the plate is at its equilibrium position Δx_{min}, but if it is given enough of a push to overcome the energy barrier ΔU to the right, it enters a region where the net force is in the same direction as its motion causing the plate to accelerate until it crashes into the sense plate. The size of the push, which is the kinetic energy imparted by the sense pulse, determines whether pull-in takes place. The fact that dynamic pull-in can occur during the damping portion of the measurement cycle imposes a further restriction on the maximum sense voltage $V_{S,max}$, and hence an additional sensitivity limit. As the damping voltage V_D increases toward the static pull-in voltage V_{PI}, which is the point at which the energy barrier ΔU disappears (Figure 2.8), we see that the sense voltage $V_{S,max}$ must go to zero to prevent dynamic pull-in. When the resistor R_D is non-zero the voltage V_G changes with time, and numerical simulation is required to determine the voltage relationship between V_D and $V_{S,max}$.

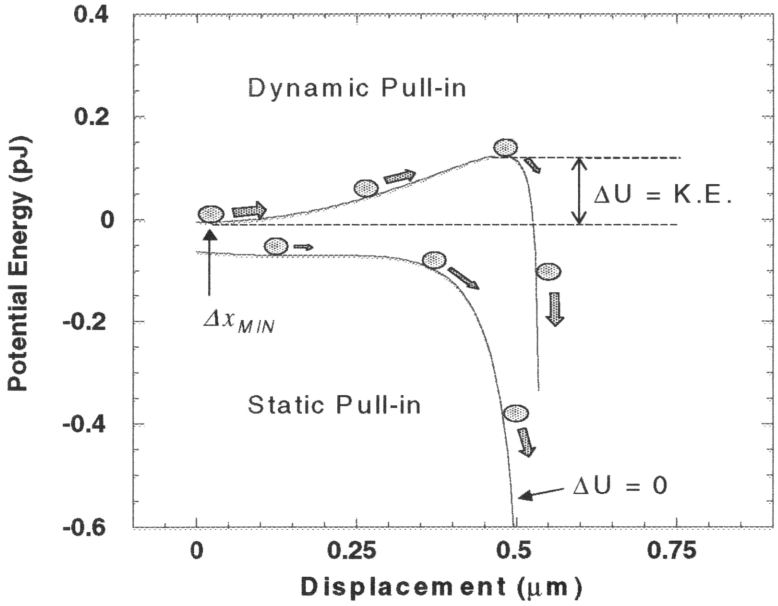

Figure 2.7: Potential Energy functions for Dynamic Pull-in and Static Pull-in. ΔU is a measure of the "energy barrier" that must be overcome for dynamic pull-in to take place. Δx_{MIN} is the stable equilibrium position. Static pull-in occurs when ΔU is zero, when no stable equilibrium exists.

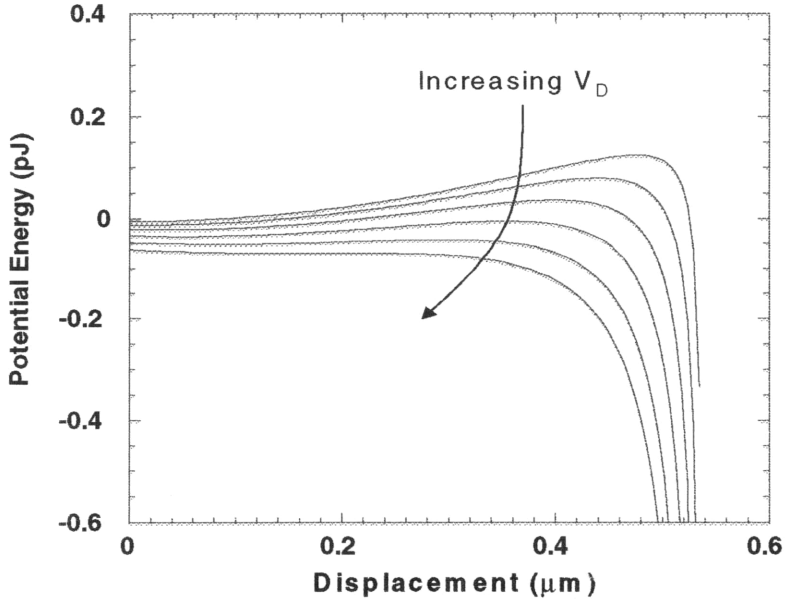

Figure 2.8: Potential energy functions for various damping voltages. The potential energy barrier decreases as V_D approaches the static-pull in voltage.

2.5 Simulations

The 1-D model of the sensor is described by a pair of coupled ordinary differential equations, the first describing the motion of the elastically supported plate, and the second describing the charge flow through the resistor.

$$m\frac{d^2x}{dt^2} = K(h_0 - x) - \frac{1}{2}\frac{\varepsilon_0 A V_G^2}{x^2} \tag{2.11}$$

$$\frac{dQ}{dt} = \frac{V_D - V_G}{R_D} = \frac{V_d}{R_d} - \frac{Q}{R_d C} \tag{2.12}$$

where

$$V_G = \frac{Q}{C}, \quad C = \varepsilon_0 A\left(\frac{1}{h} + \frac{1}{x}\right) \tag{2.13}$$

m is the effective mass of the supported plate, x is the position of the supported plate, t is the time, K is the effective spring constant, h_0 is the nominal gap height, h is the static gap height, ε_0 is the permittivity of vacuum, A is the area of the plate, and Q is the charge on the sense plate. Note that the reference capacitor is chosen to match the static value of the sense capacitance $\varepsilon_0 A/h$.

MATLAB™ scripts were written to integrate these equations in time to determine the motion of the plate and flow of charge. Nominal values for the thermomechanical radiant energy sensor were used for all the simulations.

2.5.1 Optimization

The objective of optimizing a pulsed-capacitive sensor is to maximize sensitivity for a given minimum sampling rate. In a pulsed-capacitive sensor, the minimum sampling rate is equal to the time it takes to damp residual mechanical oscillations below the resolution of the sensor. When resistive damping is used, damping is optimized by judiciously choosing the damping resistance R_D and damping voltage V_D. However, because of dynamic pull-in (discussed in Section [2.4.4]), the sensitivity and damping time cannot be optimized independently. Increasing V_D to reduce the damping time means that $V_{S,max}$ must be reduced to prevent dynamic pull-in. A methodology to optimize a pulsed-capacitive sensor that uses resistive damping is presented.

As the damping problem is non-linear in nature, and no analytical solution to problem is found, optimization is performed numerically. However, the heuristic arguments presented in the previous sections are used to narrow the range over which numerical simulation is performed.

The criterion used to quantify damping is chosen to be the time taken for the residual mechanical oscillations to "settle" below an amplitude that is determined by resolution of the sensor.

Optimization is demonstrated using the thermomechanical radiant energy sensor as an example. The requirements for the minimum resolution and damping time are 0.1nm and 10ms respectively. The sense pulse width was fixed at 0.1μs.

The first step is to optimize the resistance. In Figure 2.9 the damping time is plotted against resistance for different damping voltages. Damping time decreases with damping voltage, and is minimized for particular values of damping resistance. The damping time is minimized close to the value of resistance predicted by Equation (2.9) over the range of damping voltages shown in the figure. The total capacitance C_T was equal to the sum of the nominal sense capacitance C_{S0} and the reference capacitance C_R, and the natural mechanical resonant frequency ω_0 was used for ω. The damping time is insensitive to the damping resistance around the minima. Referring to Figure 2.9, this implies that R_D may be chosen independently of V_D without significant error in the optimization. The next step, therefore, is to keep R_D fixed at the optimum value and optimize V_D and V_S. The assumption is made that the sense voltage does not affect the optimization of R_D.

For a particular V_D, the maximum sense voltage $V_{S,max}$ is uniquely determined by the dynamic pull-in limit. In Figure 2.10 $V_{S,max}$ is plotted as a function of V_D. Figure 2.10 also shows the damping time for the pair V_D, $V_{S,max}$ (V_D). That is, it shows the time taken to damp oscillations with damping voltage V_D, when $V_{S,max}$ is applied.

The damping voltage is chosen to meet the minimum damping time criteria using Figure 2.10. The corresponding maximum (and hence, optimum) sense voltage is then simply read off the plot. Thus, for the radiant energy sensor, the optimum sense voltage is 2.62V at a damping voltage of 45mV.

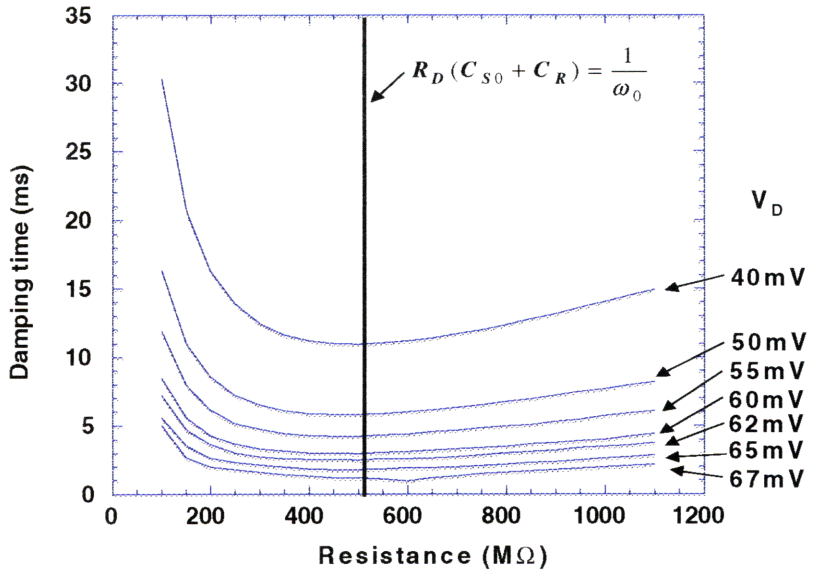

Figure 2.9: Damping time as a function of damping resistance and damping voltage. Note that the damping time is minimized around the value at which the RC time constant equal to the period of oscillation divided by 2π. Additionally, damping time is relatively insensitive to the resistance around the minimum.

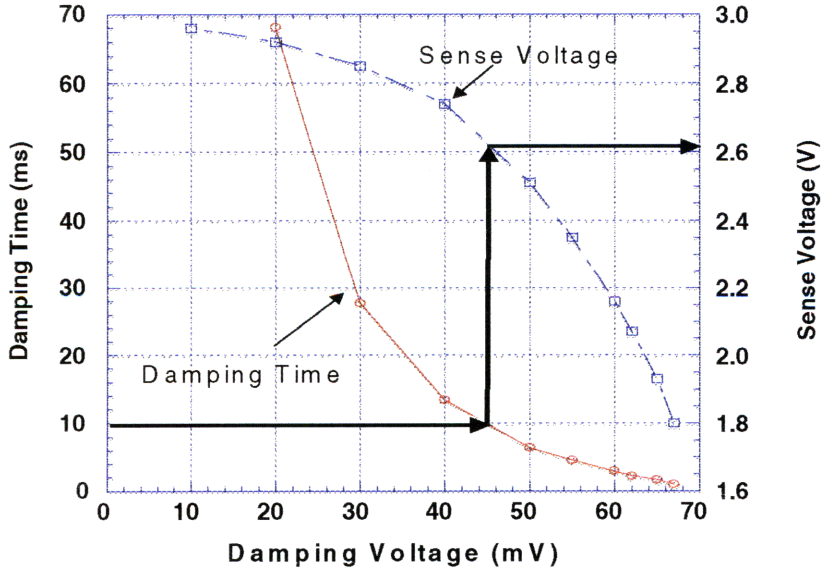

Figure 2.10: Damping time and sense voltage as a function of damping voltage. The arrows represent a route to optimizing the sense voltage, given a sampling time, or equivalently, damping time constraint.

2.5.2 Static Displacement

Figure 2.11 shows the position of the elastically supported plate over time as it is damped. The plate settles to a value less than the nominal gap height h_0.

At the end of a damping cycle, capacitors C_S and C_R are charged to a voltage V_D (Figure 2.12), and the resulting electrostatic load on the elastically supported plate causes a static displacement from the nominal gap h_0 reducing the static gap height to h. Thus, the static value of sense capacitance is greater than the nominal value of sense capacitance. Referring to Equation (2.1) the smaller static gap height means that the reference capacitor C_R must be chosen to match the static sense capacitance $\varepsilon_0 A/h$ and not the nominal sense capacitance $\varepsilon_0 A/h_0$ (C_{S0}). Otherwise, the output of the differential sensing scheme would be non-zero when no stimulus is applied to the sensor (assuming the sense pulses are balanced). The normalized static gap height h/h_0 is plotted against the damping voltage in Figure 2.13. If V_D is above the static pull-in voltage V_{PI}, the system is unstable and the supported plate collapses. Therefore, the damping voltage must be below V_{PI}.

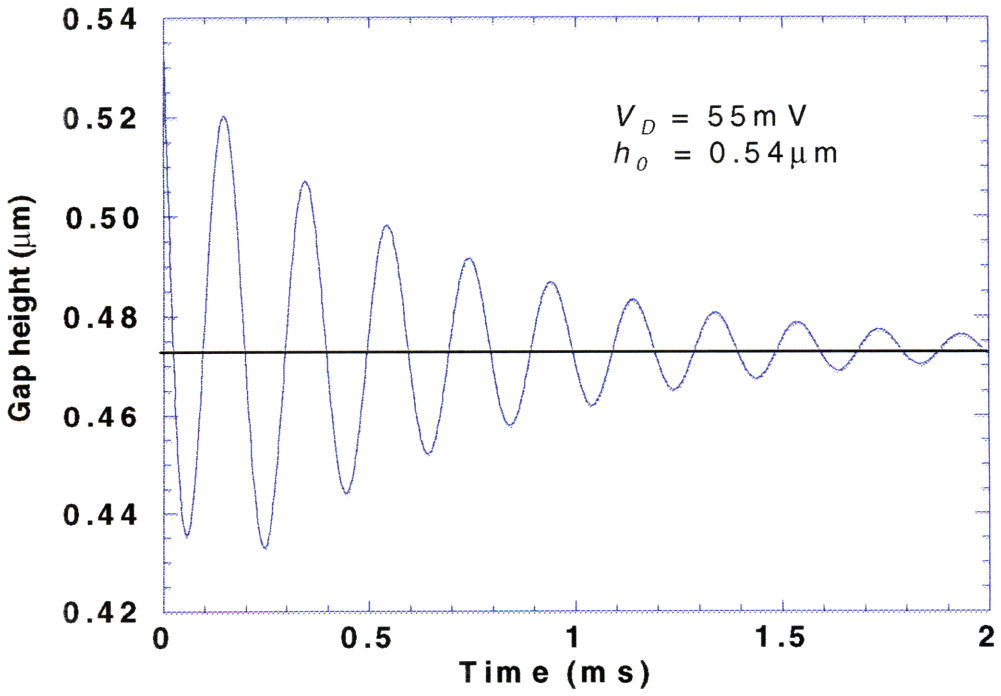

Figure 2.11: Graph of gap height during damping. The plate settles to a height less than the nominal gap height h_0.

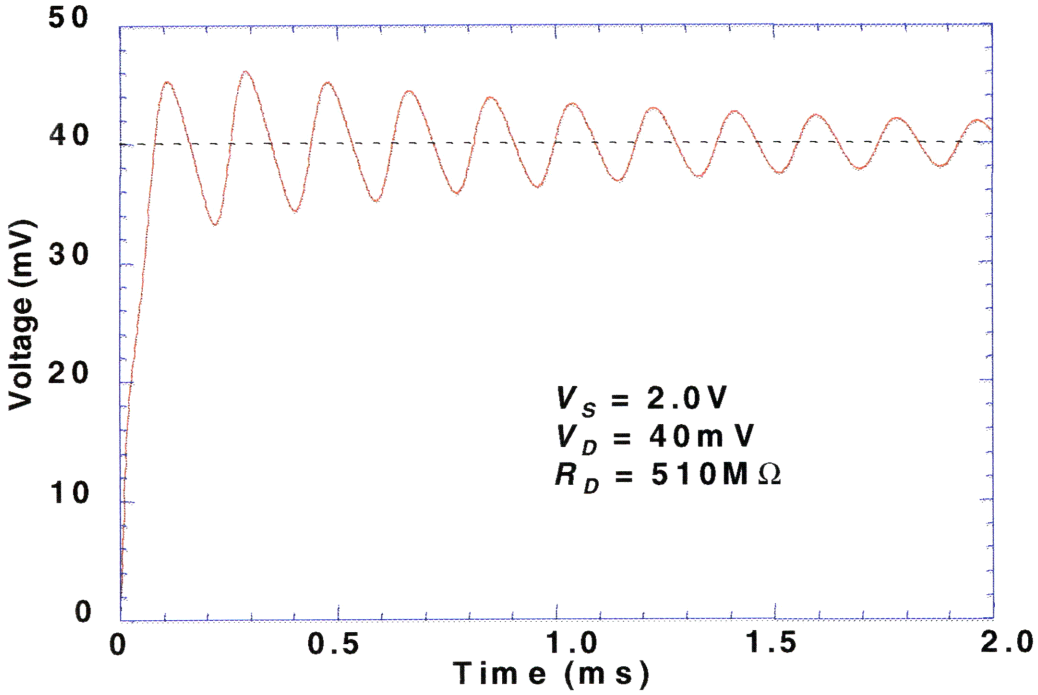

Figure 2.12: The voltage on the sense plate settles to the damping votlage V_D.

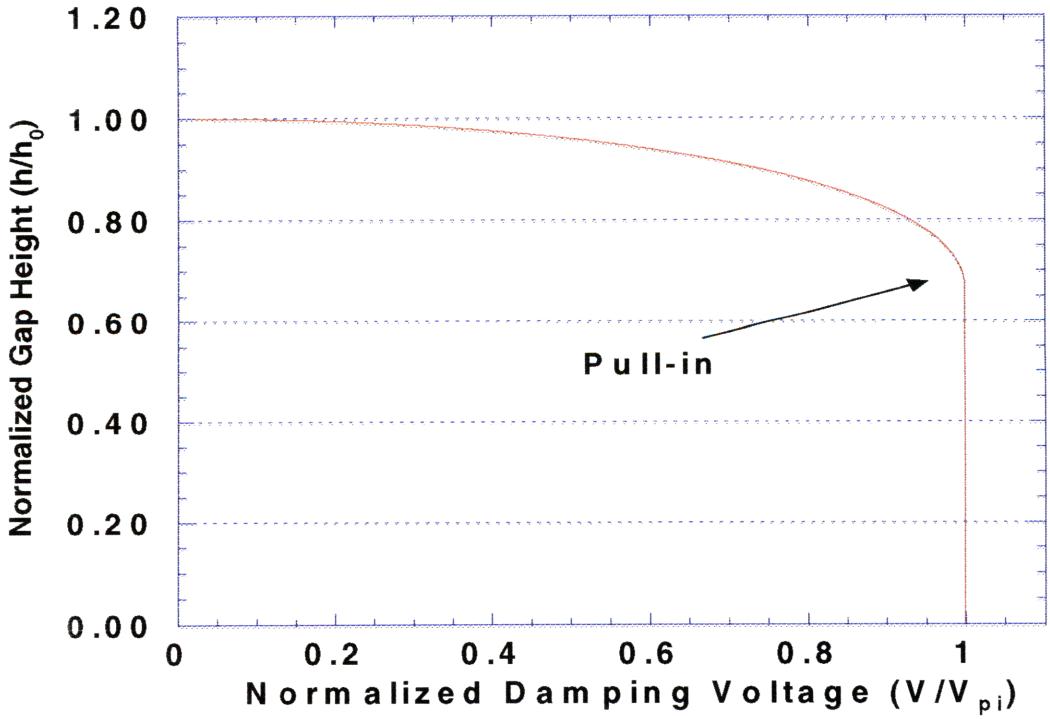

Figure 2.13: Normalized gap height plotted against the normalized damping voltage. The pull-in instability occurs when the plate is displaced by one third of the nominal gap height.

CHAPTER 3

Experimental Results

In this chapter, experimental verification of resistive damping is presented and its dependence on the damping resistance is demonstrated. In the experiments, an aluminum diaphragm is used to represent the elastically supported capacitive plate of a microelectromechanical position sensor. The diaphragm is excited into mechanical oscillation using a voltage pulse, and the oscillations are then damped resistively.

3.1 Setup

The micro-machined aluminum diaphragm used for the measurements was fabricated by Texas Instruments [11], and is shown in Figure 3.1. It has a diameter of 600μm, a resonant frequency of 240kHz, a pull-in voltage of 11.8V, and a gap height of 1.49μm. It forms the top plate of a capacitor C_S which is placed in the current integration circuit shown in Figure 3.2. The idea is to use the displacement current *d(CV)/dt* through the diaphragm capacitor to measure mechanical oscillations in the diaphragm. For small amplitude displacements, the output voltage is proportional to the displacement (Appendix A). Switch A permits a resistor to be inserted between the voltage source and the diaphragm so that the effects of resistive damping can be measured. The entire circuit is placed in a vacuum bell jar and experiments are performed under vacuum, at a pressure of about 0.01 mbar to eliminate the effects of squeeze film damping (see Figure 3.3).

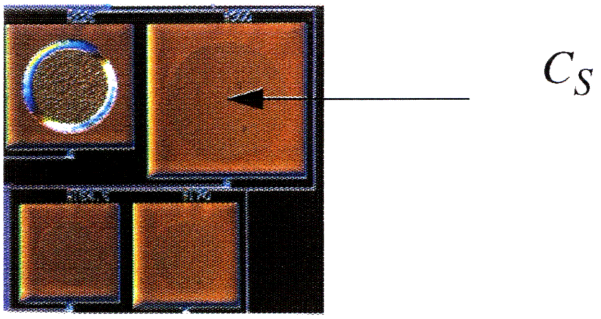

Figure 3.1: Photograph of the Texas Instruments surface micromachined aluminum circular diaphragm. The diaphragm on the top right is used in all the measurements. It has a diameter of 600μm, a thickness of 0.45μm, and is suspended 1.49μm above a ground plane. The diaphragm on the top left is pulled in.

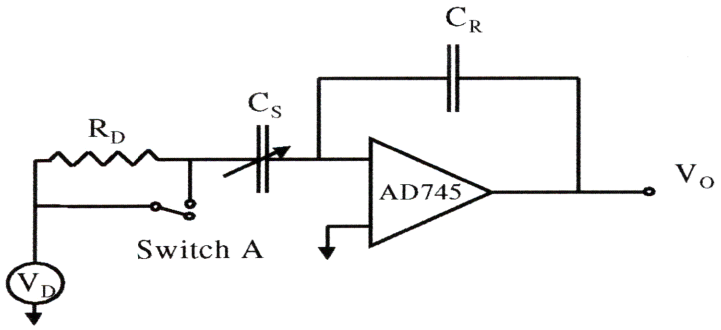

Figure 3.2: Integrator used to measure capacitive changes in C_S.

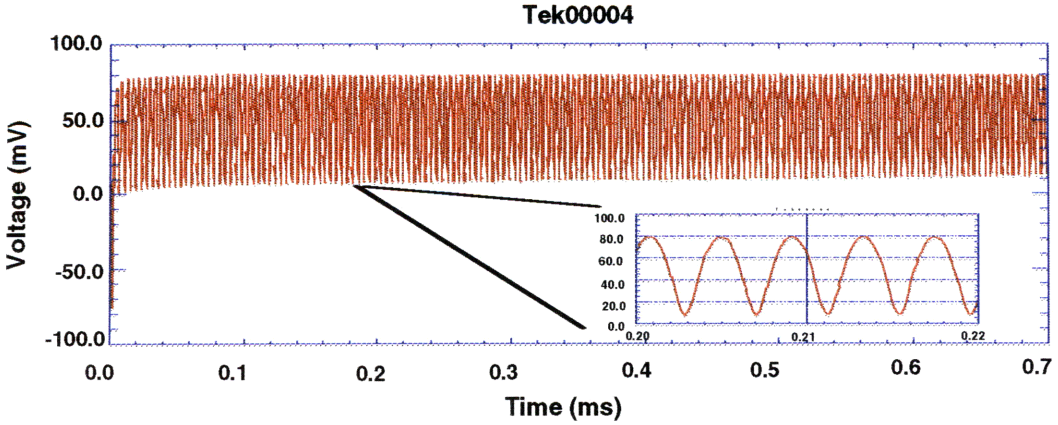

Figure 3.3: The plot above shows the output of the opamp after the diaphragm is set in motion with a voltage pulse when resistive damping is not used. Any damping is assumed to be the result of intrinsic mechanical damping of the resonator, or possibly CSQFD from residual gas. This experiment verifies that at a pressure of about 0.01mbar, there is only a small damping effect on the diaphragm over the time period of interest (~1ms).

The circuit in Figure 3.2 uses an AD745 (20MHz unity gain bandwidth) opamp with a reference capacitor of 40pf. A smaller capacitor can be used to improve the gain of this circuit, but will compromise its bandwidth. With the switch closed, and a DC bias applied, any change in the diaphragm capacitance causes current to flow. The charge that flows is equal to $\Delta C_S(t)V_D$, and this appears as a voltage $\Delta C_S(t)V_D/C_R$ at the output of the opamp. The output of the opamp is therefore proportional to the changes in charge on the sense plate.

3.2 Measurement

Applying a voltage pulse at V_D, when switch A is closed, imparts kinetic energy to the diaphragm which begins to oscillate. When switch A is opened, the resistor R_D falls between the voltage source and the diaphragm, with the DC bias acting as a damping-voltage. The results for well chosen values of damping voltage and resistance is shown in Figure 3.4.

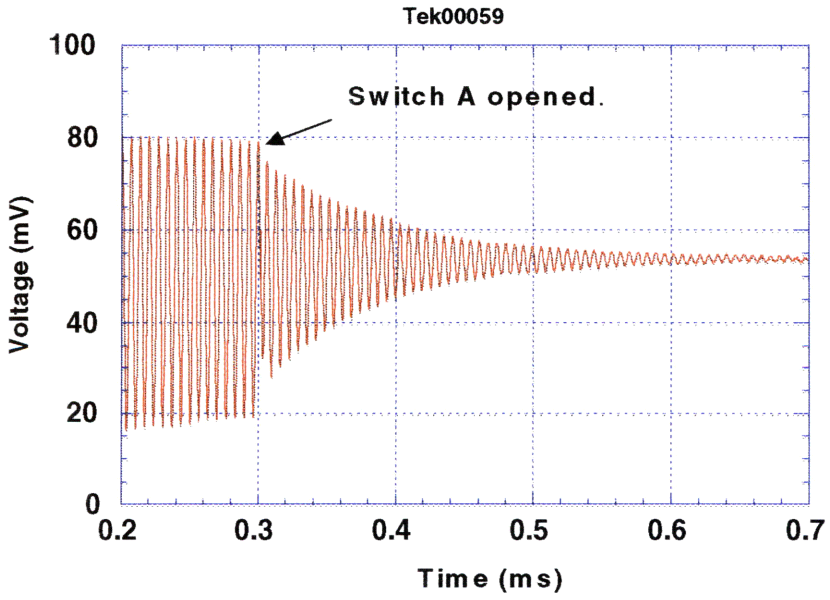

Figure 3.4: Opamp output during damping.

3.2.1 Damping as a Function of Resistance

For small amplitudes, the motion of the elastically supported plate is approximately a damped sinusoid given by

$$x(t) = Ae^{-t/\tau}\sin(2\pi ft + \phi) + h \tag{3.1}$$

where A is the amplitude of motion, τ is the damping time constant, f is the frequency of oscillation, ϕ is a phase constant, and h is the gap height. Additionally, it is shown in Appendix 1 that the damping time constant τ in Equation (3.1) is equal to the damping time constant of the charge oscillations on the capacitor. Now, because the output of the opamp is proportional to the changes in the charge τ can be determined by fitting a damped sinusoid to the output of the opamp and extracting the damping time constant.

Figure 3.5 shows the measured relationship between the damping time constant and resistance at a fixed damping voltage. The damping time constant is minimized for a particular value of resistance which is consistent with Equation (2.9), repeated here

$$R_D C_T \approx \frac{1}{\omega_0} \tag{3.2}$$

where R_D is the damping resistance, C_T is the total capacitance (including parasitic) seen by the resistor, and ω_0 is the natural resonant frequency. Measured values for C_T and ω_0 are 40pf and 1500krad/sec, respectively. The optimum value of R_D predicted from Equation (3.2) is17kΩ, close to the measured optimum of 25kΩ. Figure 3.5 also shows simulation results based on the theory presented in Chapter 2. All simulations were performed using a circuit simulator based on SPICE3[12].

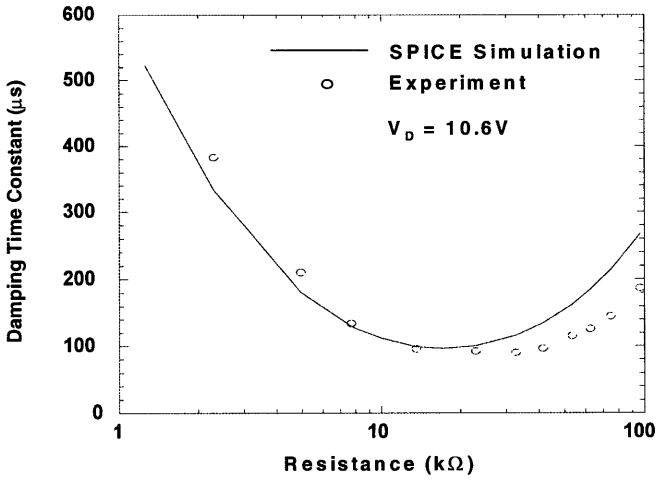

Figure 3.5: Comparison of simulated and measured damping time constants.

CHAPTER 4

Summary and Conclusions

Pulsed capacitive sensors allow the use of sense voltages significantly higher than the static pull-in voltage in a differential capacitive measurement. This is particularly beneficial in microelectromechanical capacitive sensors that are limited in their sensitivity by the instability known as pull-in. As the sensitivity of differential measurement schemes is proportional to the sense voltage, a higher sense voltage improves the sensitivity of a measurement.

Pulsed capacitive sensing is an inherently dynamic technique that samples changes in capacitance over time. The maximum sampling rate is determined by the method used to damp mechanical oscillations that result from a measurement. Thus, the method used to damp oscillations is a critical component of this measurement technique.

Compressible squeeze film damping (CSQFD) is possible for sensors that do not operate in vacuum, and can improve the sensitivity and sampling rate of a pulsed-capacitive sensor from what is possible in vacuum. However, there are sensors that must operate in vacuum, and for these sensors resistive damping is shown to be an effective damping method. This damping method is not limited in its use to pulsed-capacitive sensors and can be extended to applications involving elastically supported capacitive structures, such as pressure sensors and accelerometers. The use of CSQFD and the extension of resistive damping to other applications are interesting topics for further investigation.

The resistor and DC damping voltage used in resistive damping must be optimized numerically. However, some heuristic arguments are presented to aid in the optimization process. The resistance is optimized around the value at which the RC time constant of the electrical circuit matches the period of mechanical oscillation divided by 2π. The damping voltage is then chosen to satisfy the minimum sampling rate criterion of the particular sensor.

Resistive damping introduces a limitation on the sensitivity of a pulsed capacitive sensor because of the effect of dynamic pull-in that can potentially "crash" the sensor. It limits the maximum sense voltage that can be applied. Resistive damping also increases the static value of the sense capacitance, and this must be considered when choosing an appropriate reference capacitor in a differential capacitive measurement scheme.

Ultimately, the figure of merit of any sensing technique is the signal to noise ratio and not the raw sensitivity. The signal to noise ratio was not investigated in this thesis; however, it is an important consideration. Reducing the measurement pulse-width increases the bandwidth of the measured signal and implies a higher noise contribution from the sensing electronics. The trade-offs between pulse-width, pulse-height, and the signal to noise ratio are topics for further investigation.

References

[1] J.C. Lotters, W. Olthuis, P.H. Veltink, P. Bergveld, "Characterization of a Highly Symmetrical Miniature Capacitive Triaxial Accelerometer," Proceedings of Transducers' 97, Volume 2, pp. 1177-1180, Chicago, June 16-19, 1997.

[2] Carlos H. Mastrangelo, Xia Zhang, and William C. Tang, "Surface-Micromachined Capacitive Differential Pressure Sensor with Lithographically Defined Silicon Diaphragm," Journal of Microelectromechanical Systems, Vol. 5, No. 2, pp. 98-105, June 1996.

[3] Joseph T. Kung, and Hae-Seung Lee, "An Integrated Air-Gap-Capacitor Pressure Sensor and Digital Readout with Sub-100 Attofarad Resolution," Journal of Microelectromechanical Systems, Vol. 1, No. 3, pp. 121-129, September 1992.

[4] R. Amantea, C.M. Knoedler, F.P.Pantuso, V.K Patel, D.J.Sauer, & J.R. Tower, "An Uncooled IR Imager with 5mKelvin NEDT", 1997 IRIS Specialty Group Meeting on Passive Sensors, Tucson, AZ, 1997.

[5] M. Varghese, R. Amantea, D. Sauer, Stephen D. Senturia, "Resistive Damping of Pulse-Sensed Capacitive Position Sensors," Proceedings of Transducers' 97, Volume 2, pp. 1121-1124, Chicago, June 16-19, 1997.

[6] P.M. Osterberg, R.K. Gupta, J.R. Gilbert, S.D. Senturia, "Quantitative Models for the Measurement of Residual Stress, Poisson's Ratio and Young's Modulus using Electrostatic Pull-in of Beams and Diaphragms," Proceedings of the 1994 Solid-State Sensor and Actuator Workshop, pp. 184-188, Hilton Head, SC, June 1994.

[7] James B. Starr, "Squeeze-film Damping in Solid-State Accelerometers," Tech. Digest, IEEE Solid State Sensor and Actuator Workshop, pp. 44-47, Hilton Head Island, SC, June 1990.

[8] R. K. Gupta, E. S. Hung, Y.-J. Yang, G. K. Ananthasuresh, and S. D. Senturia, "Pull-in Dynamics of Electrostatically-Actuated Beams," Proceedings of the 1996 Solid-State Sensor and Actuator Workshop, Late News Session, pp. 3-6, Hilton Head, SC, June 3-6, 1996.

[9] Raj K. Gupta and Stephen D. Senturia, "Pull-in Time Dynamics as a Measure of Absolute Pressure," MEMS '97, pp. 290-293, Nagoya, Japan, January 26-30, 1997.

[10] W. McC. Siebert, "Circuits, Signals, and Systems," McGraw Hill Book Company, pp. 175-176, 1986.

[11] P.A. Congdon, T.-H. Lin, Texas Instruments Inc. personal communication.

[12] IsSpice4, Intusoft, San Pedro, CA.

APPENDIX A

Small Signal Analysis

An analytic approximation to the resistive damping problem is obtained under the conditions of small deflections and small charge fluctuations around their respective static values. At the end of a damping cycle, the elastically supported plate is at rest, and no current is flowing through the resistor. Under these static conditions, the voltage across the sense capacitor is V_D giving a charge $V_D/(\varepsilon_0 A/h)$ on the supported plate, where h is the static gap height. The charge applies an electrostatic load on the plate making h less than the nominal gap height h_0 of the sensor.

Linearizing Equations (2.10) and (2.11) around the static position h and static charge on the sense plate $V_D/(\varepsilon_0 A/h)$, we obtain

$$m\frac{d^2}{dt^2}\Delta x = \left(-K + \frac{C_S C_R V_D^2}{(C_S + C_R)h^2}\right)\Delta x + \frac{C_S V_D}{(C_S + C_R)h}\Delta q \tag{A.1}$$

$$\frac{d}{dt}\Delta q = -\left(\frac{V_D}{R_D h} - \frac{C_R V_D}{R_D(C_S + C_R)h}\right)\Delta x - \frac{1}{(C_S + C_R)R_D}\Delta q \tag{A.2}$$

where Δx and Δq are the perturbations of position and charge respectively, C_S is the static sense capacitance, C_R is the reference capacitance, R_D is the damping resistance, and V_D is the damping voltage. Under initial conditions, of Δx=0, Δq=0, and $d\Delta x/dt = v$, where v is a velocity, these equations can be solved using the Laplace transform.

$$\Delta X(s) = \frac{mv\left(s + \dfrac{1}{(C_S + C_R)R_D}\right)}{s^3 + \dfrac{1}{(C_S + C_R)R_D}s^2 + \omega_{EFF}^2 s + \dfrac{1}{(C_S + C_R)R_D}\omega_S^2} \tag{A.3}$$

where

$$\omega_S^2 = \frac{1}{m}\left(K - \left[\frac{C_S V_D^2}{h^2}\right]\right) \tag{A.4}$$

and

$$\omega_{EFF}^2 = \frac{1}{m}\left(K - \frac{C_R}{(C_S + C_R)}\left[\frac{C_S V_D^2}{h^2}\right]\right) \tag{A.5}$$

ω_S and ω_{EFF} are identified as the frequencies of oscillation when the damping resistor is very small, and very large respectively. Finally,

$$\Delta Q(s) = \frac{m\omega_{EFF}^2 \Delta X(s)}{R_D\left(s + \frac{1}{(C_S + C_R)R_D}\right)} \tag{A.6}$$

Note that ΔX(s) and ΔQ(s) have identical denominators and therefore have the same poles. Without explicitly solving for the Δx and Δq in the time domain the general form of the physical variables can be deduced. First, we determine if the system is stable by applying the Routh test [10] to determine if all the poles of the system are in the left half plane. The poles of the system are given by the roots of the denominator of Equation (A.3). According to the Routh test, the necessary and sufficient conditions for the roots of a cubic equation, $s^3 + \alpha s^2 + \beta s + \gamma$, to lie in the left half plane are $\alpha, \beta, \gamma > 0$ and $\beta > \gamma/\alpha$. Examining Equation (1.3) we identify

$$\alpha = \frac{1}{(C_S + C_R)R_D} \tag{A.7}$$

$$\beta = \omega_{EFF}^2 \tag{A.8}$$

$$\gamma = \frac{1}{(C_S + C_R)R_D}\omega_S^2 \tag{A.9}$$

The first condition $\alpha, \beta, \gamma > 0$ holds as long as ω^2_{EFF} and ω^2_S are greater than zero. Inspection of Equation (A.4) shows that ω^2_S is positive as long as $K > C_S V^2_D / h^2$. This is true if V_D is less than the pull-in voltage V_{PI}. Using Equation (2.5) it can be shown that $C_S V_D^2/h^2$ is just equal to K at pull-in. Inspection of Equation (A.5) shows that ω^2_{EFF} is greater than ω^2_S because $C_R/(C_R + C_S)$ is less than 1. Therefore ω^2_{EFF} is also positive.

For the second condition $\beta > \gamma/\alpha$ to hold true

$$\omega_{EFF}^2 > \frac{\frac{1}{(C_S + C_R)R_D}\omega_S^2}{\frac{1}{(C_S + C_R)R_D}} \tag{A.10}$$

Expanding ω^2_{EFF} and ω^2_S and re-arranging the in-equality, the condition simplifies to

$$\frac{C_R}{(C_S + C_R)} < 1 \tag{A.11}$$

which must be true as C_S and C_R are both positive. Summarizing the results of the two tests, as long as V_D is less than the pull-in voltage the system is stable. This implies that $\Delta x(t)$ and $\Delta q(t)$ decay in time. Now, Equation (A.6) shows that the $\Delta Q(s)$ and $\Delta X(s)$ have the same poles, therefore, $\Delta q(t)$ and $\Delta x(t)$ must have the same decay time constants.